

## 12.6 A Power-Efficient Voltage-Based Neural Tissue Stimulator with Energy Recovery

Shawn K. Kelly and John Wyatt

Massachusetts Institute of Technology, Cambridge, MA

Neural and muscular tissue stimulators are used in cochlear implants, cardiac pacemakers, and other medical implants[1][2]. Nearly all of these stimulators use a linear current source to drive electrodes with a charge-balanced biphasic current pulse. This method consumes high levels of power, limiting battery life and exposing tissue to potentially damaging temperatures. This is especially true for retinal prostheses, which motivate this design. An efficient neural tissue stimulator is designed using a voltage-based drive. This system, which includes wireless power transmission to the implant, achieves a 53% reduction in power compared to efficient traditional linear current sources.

Figure 12.6.1 shows a system block diagram. In any such implant, major power dissipation occurs in three areas: the electrodes, the power circuitry driving the electrodes, and the secondary coil. Power consumption in the electrodes is  $I^2R$  loss, largely in the fluid and tissue. The traditional current source minimizes this loss with constant current drive. This design approaches the minimum power consumption by driving electrodes with a sequence of voltage steps, charging the electrode metal-fluid capacitance. In the power path circuitry, traditional current-source drivers dissipate substantial unnecessary power in the linear-mode output transistor. Power consumption in the path is minimized in this design by supplying charge to the electrode directly from intermediate voltage supplies (closer to the electrode voltage than  $V_{dd}$  and  $V_{ss}$ ), and rectifying directly from the secondary coil to those supplies. Finally, power consumed in the secondary coil is  $I^2R$  loss. By using synchronous rectification to draw current from the secondary when its voltage is near the intermediate sources, the coil current is extended in time, while the traditional method uses a standard rectifier, conducting all required current in short-duration, high-current spikes at the voltage peaks.

Iridium oxide is increasingly used for stimulation electrodes and its impedance consists of an electrode-fluid interface capacitance in series with a fluid resistance. Capacitances are measured, for 400 $\mu$ m diameter electrodes, ranging from 0.3 $\mu$ F to 3.0 $\mu$ F, and resistances from 1.1k $\Omega$  to 2.5k $\Omega$ . The electrodes used here are measured as 0.49 $\mu$ F and 2.3k $\Omega$ . Driving electrodes with a biphasic current pulse as shown in Fig. 12.6.2 results in the voltage waveform shown. The required charge may be delivered with less power than is used in a traditional current source if the electrodes are driven with a voltage source which exactly follows the voltage waveform in Fig. 12.6.2. Switching the electrode through a sequence of increasing voltage steps approximates this voltage-based drive. However, this requires efficient generation and maintenance of these intermediate voltage sources. The synchronous rectifier in Fig. 12.6.1 achieves this, drawing current from the secondary coil when its voltage is near the intermediate supply capacitor voltage. Five 1 $\mu$ F capacitors form the voltage network, and are charged to target voltages provided by a reference circuit. Digital control circuitry switches the 15 electrodes to the appropriate supply capacitors.

Figure 12.6.3 shows the synchronous rectifier charging the capacitor network, which drives the electrodes and is driven by them upon electrode discharge. The synchronous rectifier is critical to this design, since its efficiency determines much of the system power consumption. As shown in Fig. 12.6.4, the syn-

chronous rectifier consists of a continuous comparator to monitor the 125kHz ac voltage, a clocked comparator to ensure that the capacitors reach their target voltages, and circuitry to control rectifier timing. The switch turns on for 400 or 800ns if the capacitor being charged is lightly loaded with few electrodes, or for a longer duration ( $>1\ \mu$ s) if the capacitor is loaded with many electrodes. The continuous comparator uses Bazes' VCDA[3], but with a predictive front end with first-order current cancellation which varies the dc voltage seen by the amplifier based on the slope of the incoming ac voltage[4]. This results in a delay of 40ns and consumption of 54 $\mu$ W.

The chip is tested with the full wireless power system with the primary driven by a class E amplifier, and with electrodes in saline with a platinum return. Electrode current is measured with an instrumentation amplifier with a gain of 400 across a 10 $\Omega$  series resistance. Figure 12.6.5 shows the stepwise voltage and current waveforms measured for an electrode. Power is determined from the voltage across and current through the secondary coil. Voltage is measured with a unity gain instrumentation amplifier and current with an instrumentation amp of gain 500 across a 0.5 $\Omega$  resistor. Power consumed within the coil is calculated from the coil resistance and current and added to the total. The measured coil current and voltage waveforms in Fig. 12.6.6 show surges of current charging a capacitor.

The total power consumed by the secondary system with no electrodes is 338 $\mu$ W; with 15 electrodes driven to 0.68 $\mu$ C in 5ms, discharged in 5ms, and repeated at 100Hz dissipation is 2.22mW. Thus the 15 electrodes consume 1.88mW, or 125 $\mu$ W per electrode, including the secondary coil and all power path circuits. A linear dual-supply current source supplying the same charge at 136 $\mu$ A from supply voltages of  $\pm 1.75$ V (representing a very aggressive design - many implants use  $\pm 5$ V or more), consumes 271 $\mu$ W per electrode, including coil and rectifier power. Thus, this system represents at least a 53% reduction in power from an efficient example of the traditionally used stimulation systems.

With the exception of the coil, Schottky diodes, and supply capacitors, this entire system was implemented on a 1.5 $\mu$ m CMOS chip as shown in Fig. 12.6.7.

### Acknowledgments:

Authors thank David Perreault, Rahul Sarpeshkar, Luke Theogarajan and Mariana Markova for their design insights. Support was provided by the Catalyst Foundation fellowship and NSF grant BES0201861; MOSIS provided fabrication.

### References:

- [1] B. Ziaie, et. al., "A Single-Channel Implantable Microstimulator for Functional Neuromuscular Stimulation," *IEEE Biomed. Eng.*, vol. 44, no. 10, pp. 909-920, Oct. 1997.
- [2] W. Liu, et. al. "A Neuro-Stimulus Chip with Telemetry Unit for Retinal Prosthetic Device," *IEEE J. Solid-State Circuits*, vol. 35, no. 10, pp 1487-1497, Oct. 2000.
- [3] M. Bazes, "Two Novel Fully Complementary Self-Biased CMOS Differential Amplifiers," *IEEE J. Solid-State Circuits*, vol. 26, no. 2, pp. 165-168, Feb. 1991.
- [4] A.C.H. MeVay, R. Sarpeshkar, "Predictive Comparators with Adaptive Control," *IEEE TCAS II, Ana. and Dig. Sig. Proc.*, vol. 50, no. 9, pp. 579-588, Sep. 2003.

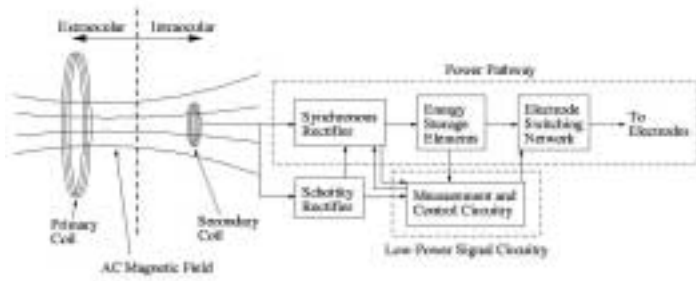


Figure 12.6.1: Stimulation system block diagram

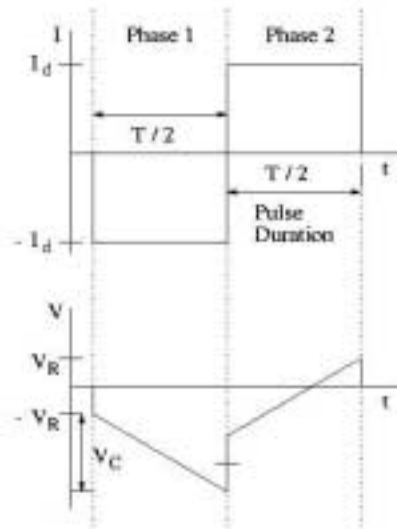


Figure 12.6.2: Stimulation current and voltage waveforms

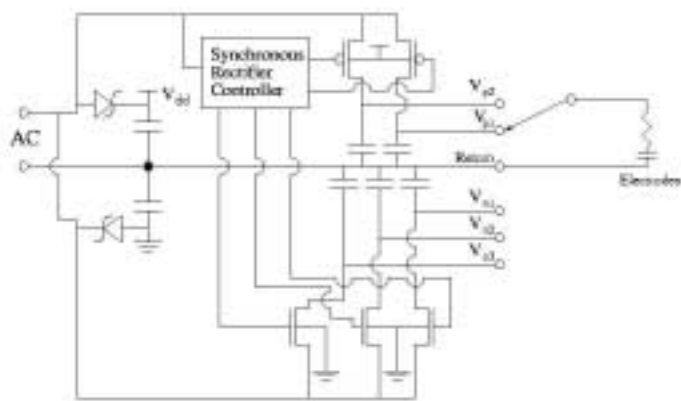


Figure 12.6.3: Synchronous rectifier block diagram

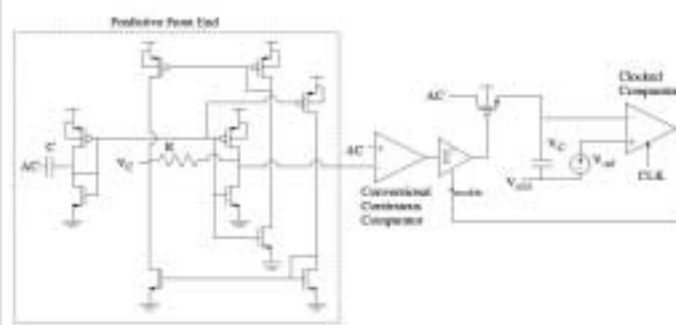


Figure 12.6.4: Synchronous rectifier circuitry

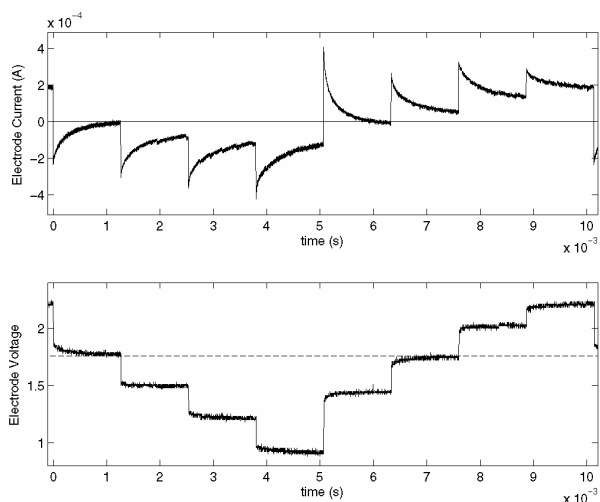


Figure 12.6.5: Measured electrode current and voltage

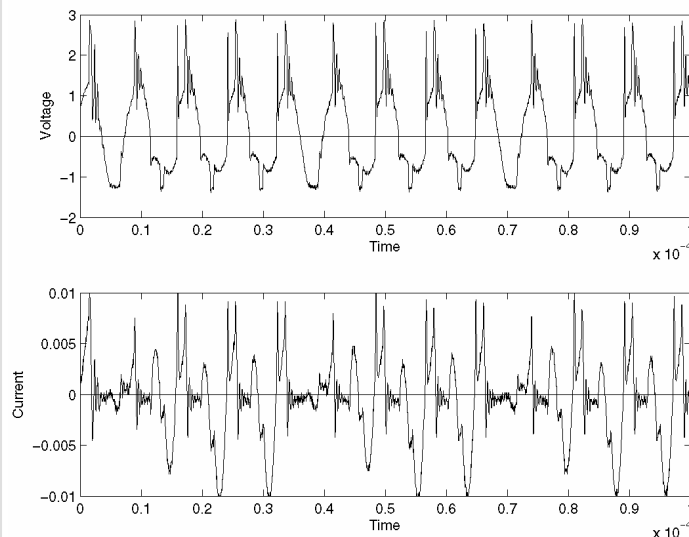


Figure 12.6.6: Secondary coil current and voltage

Continued on Page 000

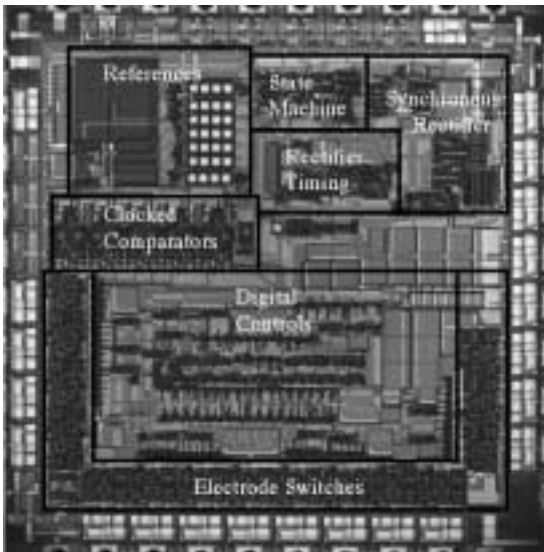


Figure 12.6.7: Chip micrograph